2007 IEEE International Conference on
Robotics and Automation
Roma, Italy, 10-14 April 2007

STRIDE: A Highly Maneuverable and Non-Tethered Water Strider Robot

Yun Seong Song and Metin Sitti

Abstract— **Recently, a few water strider robots that mimic the static and dynamic key characteristics of the insect water striders have been reported in the literature. These robots either lacked mobility or was tethered to an external source of power. Using the recent findings on the supporting legs of these robots creating repulsive surface tension based lift forces, a heavier yet highly maneuverable and non-tethered water strider robot, called STRIDE, is proposed in this paper. STRIDE uses two miniature DC motors and a lithium-polymer battery that are connected to the driving circuit on-board. Optimal leg shape is manufactured by bending 0.33 mm diameter stainless steel wires with a Teflon® coating. This 6.13 gr non-tethered robot with twelve supporting legs demonstrated a linear motion of 8.7 cm/s and a rotational motion of 0.8 rad/s. STRIDE would have potential applications in continuous water quality monitoring on lakes, dams, and other water sources and in entertainment and education in the near future.**

I. INTRODUCTION

Inspiration by nature has enabled alternative design ideas for new materials, structures, systems, and control and communication methods since the beginning of the human history. Biological systems have evolved to find just-good-enough solutions to survive. By understanding and adapting the underlying principles of these solutions at the small scales to robotic systems, many new miniature robots which can operate in unstructured environments robustly and efficiently have been proposed. Especially considering the unknowns and complexity of the physics and dynamics at the small scales, biological inspiration could have a significant inspiration source to develop and start new miniature robot designs. On the other hand, the developed bio-inspired micro/nano-robots would be used to improve our understanding of biological systems at the small scales.

Many bio-inspired robots with various mobility capabilities have been proposed in the literature. Walking and running robots [1], [2], [3] inspired by cockroaches, flapping wings based flying robots [4], [5], [6] inspired by flies, bats, and birds, surface climbing robots inspired by geckos [7], [8], [9], underwater swimming robots inspired by fishes [10], amphibious running robots inspired by basilisk lizards [11] are such example bio-inspired miniature robots. Due to the scaling effects, these miniature robots are expected to be faster, robust against shock, light, and highly maneuverable.

Y. S. Song was with the NanoRobotics Laboratory, Department of Mechanical Engineering, Carnegie Mellon University, and is now with the Department of Mechanical Engineering, Massachusetts Institute of Technology, Boston, USA. E-Mail: yssong@cmu.edu.

M. Sitti is with the NanoRobotics Laboratory, Department of Mechanical Engineering and Robotics Institute, Carnegie Mellon University, Pittsburgh, PA 15213, USA. E-Mail: sitti@cmu.edu.

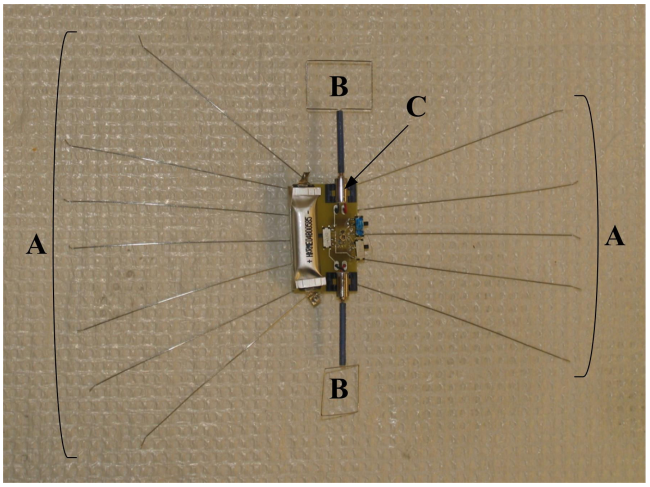

Fig. 1. Photo of the fabricated robot, STRIDE: **A** are the supporting legs, **B** are the actuating legs, and **C** is the body with on-board electronics.

As a new unique example of taking advantage of scaling effects on robotic mobility, recently, water strider inspired robots have been proposed for walking on water [13], [14], [12]. Hu *et. al.* [12] built the first synthetic water strider robot with elastic energy storage, and Suhr *et. al.* [13] built the first controllable robot on water using three piezoelectric unimorph actuators. These robots weigh less than 1 gram. Detailed modeling and analysis on the physics of these robots are conducted in [14] and [15], enabling a design methodology for building heavier and faster robots on water surface.

Though the former controllable robot was successful in demonstrating maneuverability on the surface of water, it was slow (less than 3 cm/s) and difficult to handle [13]. Moreover, the robot has to be tethered to an external signal generator due to high voltage signals required for actuating the three piezoelectric unimorphs. This tether caused many issues for the mobility of such a small and low drag robot. Therefore, this work proposes a new robot called STRIDE (Surface Tension Robotic Insect Dynamic Explorer) which uses miniature motors and on-board power source to develop a non-tethered water strider robot with higher maneuverability. Major challenge of this new non-tethered robot is to lift the increased overall robot weight which is up to 6-8 gr. Using the supporting robot leg design study of the authors with an optimal leg shape in [15], more number of legs with optimized shape is proposed to increase the lift capability of the robot. Thus, twelve legs with 7 cm length are used in this

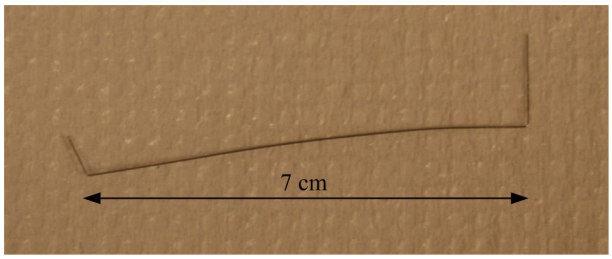

Fig. 2. Photo of the fabricated supporting leg with an optimum shape.

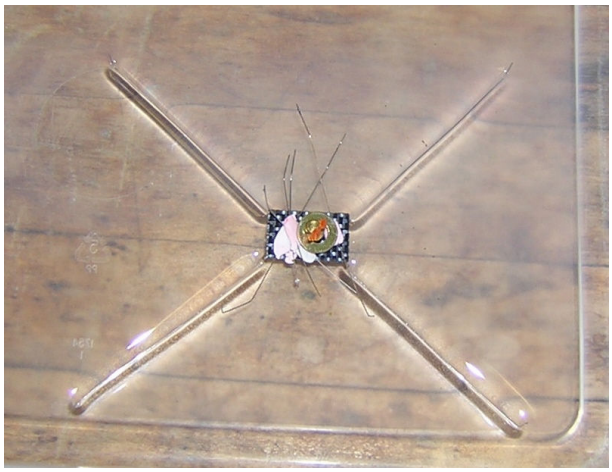

Fig. 3. Photo of the prototype with four supporting legs carrying a 3.7 gram payload.

study to lift up to 9.3 gr weight which is sufficient to include all required on-board motors, power source and circuitry. The new motion mechanism of STRIDE with two miniature motors is introduced in this paper, and the corresponding design issues and experimental results are discussed. Each feature of this robot as shown in Figure 1 is explained in detail in the following sections.

II. Supporting the Weight

As noted earlier, the previous water strider robots were light in weight (less than a gram). Lack of proper means to support heavier payload constrained them to use only light weight actuators such as piezoelectric unimorphs. For example, in [13], a supporting leg could carry no more than 0.5 grams. Then studies on how to increase the payload of the supporting legs effectively are presented in [14] and [15]. A highlight in these studies include how to find the optimal shape of the supporting leg to maximize the overall payload, given a specific leg material and diameter. From the static analysis in [15], having many 7 cm-long Teflon® coated stainless steel wires with the diameter of 0.33 mm and the optimum shape are used to support the weight of the robot. According to [15], a leg like this is expected to carry almost a gram of payload. Figure 2 shows a fabricated supporting leg with the optimum shape. Using four of these legs, a 3.7 gram payload is supported as shown in Fig. 3.

This motorized robot is expected to carry two miniature motors of nearly 1 gram each, a lithium-polymer battery

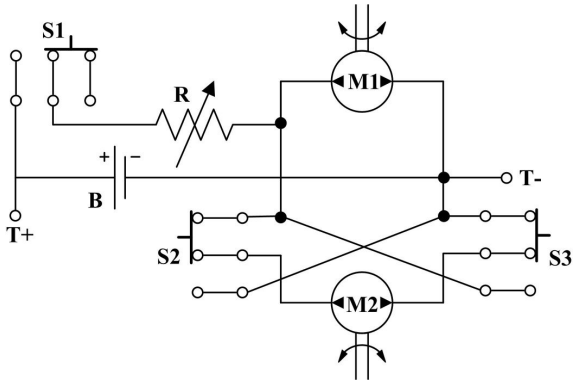

Fig. 4. The circuit diagram for the motion mechanism. The labels on the components are explained in Table I.

(Kokam) of approximately 2 grams, and some basic electronic parts on a PCB board. The weight of the robot is then expected to be at least 5 grams. Since it is experimentally shown that one supporting leg can carry about 0.8 grams, at least seven of these legs are expected to be used. The size of the body of the robot must be large enough to accommodate such number of supporting legs such that they are spaced far enough for maximum performance. Here, twelve supporting legs are used, to support 6.13 grams of the body weight and a 50% safety capacity of 3.1 grams. It was experimentally shown in [15] that twelve of these legs can support up to 9.3 grams of payload.

III. Motion Mechanism

It is advantageous to use miniature DC motors because only one actuator can create a sculling motion of the actuating legs [12] while two bending piezoelectric unimorph actuators are required to create such motion. The layout of the motor driving circuit is shown in Fig. 4. To achieve high maneuverability and to minimize the payload, two micro motors (Didel MK04S-24) of 4 mm diameter (M1 and M2) are used. A Li-polymer battery (B) is used to deliver power to the motors. Two micro switches (S2 and S3) are used to switch the polarity of the inputs to one of the motors. When both of these switches are toggled, the motor M2 would change its direction of rotation. If only one of these switches are toggled, then the M2 motor will stop. A third microswitch (S1) is used as the main on/off switch. A potentiometer (R) is used to adjust the current fed into the two motors, thus changing their rotational speed. The T+ and T− terminals are for the purpose of recharging the battery. An external charger can be connected to these terminals to supply electric energy to be stored in the exhausted battery.

Figure 5 shows a motor and an actuating leg connected by a coupling. The intent of the coupling is to space the actuating leg sufficiently far away from the body, where the supporting legs are attached, so that the water waves created by the motion of the actuating legs do not affect the loading capacity of the supporting legs. The actuating leg and the coupling together is designed such that the mass center is on the axis of the rotation of the motor. This is to eliminate

TABLE I
CIRCUIT COMPONENTS IN FIG. 4

Component	Description	Model	Vendor
R	Potentiometer	652-TC22X-2-201E	Mouser
B	Li-Polymer battery	60 mAhr Kokam	BSD Micro RC
S1	On/off microswitch	103-5040-EV	Mouser
S2	Microswitch	103-5040-EV	Mouser
S3	Microswitch	103-5040-EV	Mouser
M1	Motor	MK04S-10	Didel
M2	Motor	MK04S-10	Didel
T+	Recharge terminal	N/A	N/A
T−	Recharge terminal	N/A	N/A

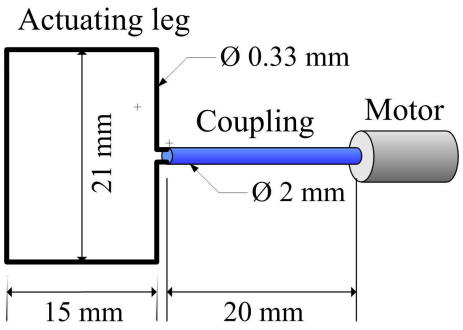

Fig. 5. Schematic of the actuation part with a motor, a coupling and an actuating leg.

any rotational imbalance during operation. It is calculated that a 1 mm offset of the 0.5 gram mass rotating about the motor axis in 20 Hz creates an instantaneous vertical load of nearly 1 gram. Two of these can be problematic since the imbalance acts as an undesired additional weight of 2 grams, forcing the robot to have at least three more supporting legs. However, this imbalance issue is not present in the case of the robot using piezoelectric unimorphs [13]. The coupling is fabricated using the rapid prototyping machine (3D Systems, Inc., Invision HR).

It is known from [15] that the Teflon® coated wires will break the surface of water when it pushes down on to it more than 3.8 mm deep. In order not to break the surface of water with the actuating legs, the leg in a rectangular shapes have width of 21 mm. This value is determined so that the actuating leg would not be pushing down on the surface of water more than 3 mm deep at any time.

The motors are attached to the motor mounts placed on the PCB board, which serves as the body of the robot. These mounts, also fabricated using the rapid prototyping machine, offsets the motor from the PCB board by 1.5 mm. With a 1.5 mm-thick PCB board and the estimated spacing between the PCB board and the water surface of 2.5 mm, the center

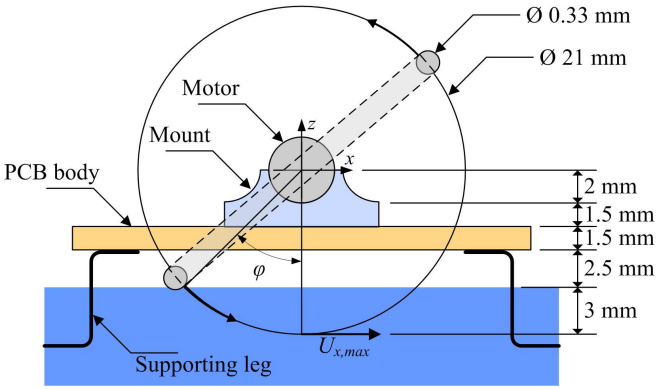

Fig. 6. Trajectory of the actuating leg and the interaction with the water surface.

of rotation for the actuating leg is expected to be 7.5 mm above the water surface (Fig. 6). Thus the actuating leg is expected not to break the surface of the water at any time during the operation.

A. Motion Analysis

From [15], the overall speed of the robot can be found from

$$p_f = \rho U'^2 A' + \mu U' \frac{A'}{w'}, \tag{1}$$

where p_f is the forward momentum generated by the actuating legs per second, U' is the overall speed of the robot, and A' and w' are the characteristic area and width of the supporting legs in total, respectively. To find p_f, the trajectory of the actuating leg is studied (Fig. 6). For one rotation (2π rad) of the motor, the fraction of time the actuating leg is in contact with the water is $4\varphi/2\pi$ (where φ is the half-sweep angle of the actuating leg trajectory). Given the maximum speed of the leg in x direction, $U_{x,max}$, where

$$U_{x,max} = 2\pi f r, \tag{2}$$

where f is the rotational frequency and r is the radius of the trajectory of the actuating leg, the average lateral speed and acceleration of the actuating leg, $U_{x,avg}$ and $\left(\frac{dU}{dt}\right)_{x,avg}$, are calculated as

$$U_{x,avg} = \frac{U_{x,max}}{\pi} \int_{-\varphi}^{\varphi} \cos\theta \; d\theta, \tag{3}$$

$$\left(\frac{dU}{dt}\right)_{x,avg} = 2\pi f U_{x,avg}. \tag{4}$$

These are used to calculate the propulsion force of the robot using the following equation [15]

$$|F| \sim \rho U^2 A + \rho g h A + \rho V \frac{dU}{dt} + \mu U \frac{A}{w} + \gamma \frac{A}{w} - \nabla \gamma A, \tag{5}$$

where w, A, and V are the characteristic width, area, and volume of the body in contact with the water (in this case,

the actuating leg), respectively, ρ is the density of water (1000 kg/m^3), g is the gravitational constant (9.8 m/s^2), h is the depth of the body into the water, μ is the viscous drag coefficient (0.89 cP), γ is the surface tension coefficient (0.072 N/m) and U is the speed of the body. Replacing $U_{x,avg}$ in place of U and taking only the significant terms from (5) [15], p_f is estimated as

$$p_f = 2\left(\rho U_{x,avg}^2 A + \rho V \left(\frac{dU}{dt}\right)_{x,avg}\right), \qquad (6)$$

since there are two motors. Taking $f = 10$ Hz, $r = 10.5$ mm, $\varphi = 0.8$ rad, $A = 4.95 \times 10^{-6}$ m^2, and $V = 1.0 \times 10^{-9}$ m^3, and applying (2)−(4) to (6), p_f is found to be 0.893 mN. Applying this value to (1) and taking $A' = 0.28 \times 10^{-3}$ m^2 and $w' = 0.33$ mm, the overall speed of robot is calculated to be around 5.5 cm/s. Since the form drag terms are dominant by 95% in (1) and (6), a simpler equation for estimating the speed of the robot can be derived as [15]

$$U' \sim \sqrt{\frac{p_f}{\rho A'}} \sim U_{x,avg}\sqrt{\frac{A}{A'}}. \qquad (7)$$

This equation yields $U' \approx$5.6 cm/s.

IV. Experiments

STRIDE is fabricated as shown in Fig. 1 and is tuned such that the motors are turning at a frequency high enough to overcome the pull back force of the water surface from the surface tension force, and low enough to not break the water surface and make splashes. The potentiometer is eventually tuned to 50 Ω in this case. The S1 switch is turned on, and the actuating legs are temporarily clamped to prevent turning. When the robot is placed on the water surface, the clamping is removed and the motors turn freely. Figures 7 and 8 shows the forward and turning motion of the robot, respectively. The turning is made possible by toggling both S2 and S3 switches. The forward speed of the robot is measured to be 8.7 cm/s, and the rotational speed is 0.8 rad/s. Battery lifetime is around 10 minutes at the maximum speed using a 60 mAhr battery.

In the forward motion experiment, STRIDE was turning slowly to the left at the same time. This may be because the M2 motor is fed in with less current than M1, due to the resistances of the S2 and S3 switches. This problem can be eliminated in the future if the two motors are connected serially to ensure same current on both motors. Another reason can be some minor fabrication errors that may have resulted in asymmetric actuating legs.

The forward speed of the robot in the experiment is 58% larger than the expectation of 5.5 cm/s. One possibility is the motors rotating faster than 10 Hz. Another possibility is the overestimated A' in (7). Since the supporting legs are lined up mostly parallel to the forward direction of the robot, the value of A' may have to be reduced greatly. Yet, the analysis in [15] and this paper on the speed of the robot yeilded a feasible value range for the overall speed.

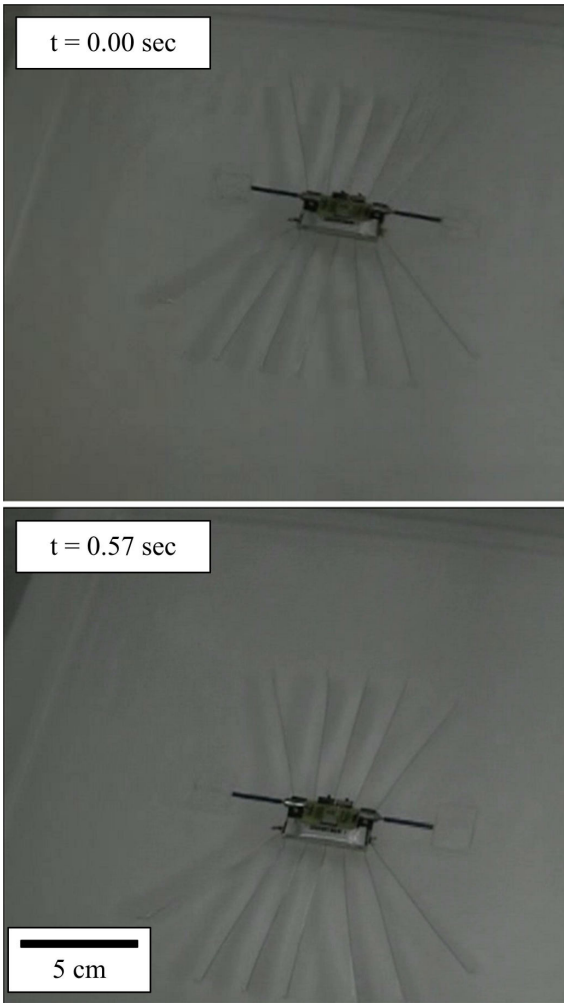

Fig. 7. Photo snapshots from the forward linear motion experiments of STRIDE with a 8.7 cm/s speed.

V. Conclusion

In this paper, a new non-tethered water strider robot, STRIDE, using two miniature DC motors and a lithium-polymer battery is proposed. Based on the analysis in [15], the number and configuration of supporting legs are decided, and the dynamics of the actuating legs is studied. The fabricated robot of 6.13 gram weight with twelve supporting legs and two motors is capable of producing a 8.7 cm/s linear motion and a 0.8 rad/s rotational motion, demonstrating the feasibility of a wireless yet agile water strider robot. In the near future, on-board electronics of the robot would be improved to include RF and infrared wireless communication capability and many motion sensors to develop single and multi-robot control applications for navigating on water surfaces autonomously. Manufacturing these autonomous robots in large numbers as a swarm robotic platform, they could be used in continuous water quality and other toxic material monitoring on water sources. Moreover, fabricated STRIDE robots and biological water striders would be used to study the social interactions between a biological insect and a robotic insect.

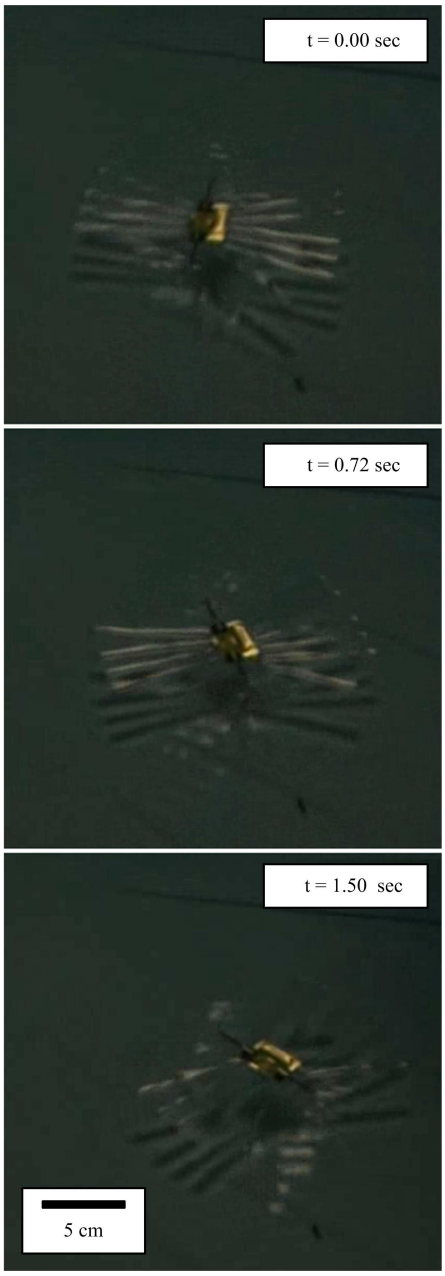

Fig. 8. Photo snapshots from the rotational motion of STRIDE with a 0.8 rad/s speed.

ACKNOWLEDGMENTS

The authors thank to Mustafa Emre Karagozler and Franklin Chung for their help on robot fabrication and experiments.

REFERENCES

[1] J. E. Clark, J. G. Cham, S. A. Bailey, E. M. Froehlich, P. K. Nahata, R. J. Full, and M. R. Cutkosky, "Biomimetic design and fabrication of a hexapedal running robot," *Proc. of the IEEE Int. Conf. on Robotics and Automation*, pp. 3643-3649, 2001.

[2] R. D. Quinn, G. M. Nelson, R. J. Bachmann, and R. E. Ritzmann, "Toward mission capable legged robots through biological inspiration," *Autonomous Robots*, vol. 11, no. 3, pp. 215-220, November 2001.

[3] U. Saranli, M. Buehler, and D. E. Koditschek, "RHex: A simple and highly mobile hexapod robot," *The International Journal of Robotics Research*, vol. 20, no. 7, pp. 616-631, 2001.

[4] R. S. Fearing, K. H. Chiang, M. H. Dickinson, D. L. Pick, M. Sitti, and J. Yan, "Wing transmission for a micromechanical flying insect," *Proc. of the IEEE Int. Conf. on Robotics and Automation*, pp. 1509-1516, 2000.

[5] T. N. Pornsin-Sirirak, Y. C. Tai, C. M. Ho, and M. Keennon, "Microbat: A palm-sized electrically powered ornithopter," *Proc. of the NASA/JPL Workshop on Biomorphic Robotics*, 2001.

[6] R. Madangopal, Z. A. Khan, and S. K. Agrawal, "Biologically inspired design of small flapping wing air vehicles using four-bar mechanisms and quasi-steady aerodynamics," *Journal of Mechanical Design*, vol. 127, no. 4, pp. 809-816, July 2005.

[7] O. Unver, A. Uneri, A. Aydemir, and M. Sitti, "Geckobot: A Gecko Inspired Climbing Robot Using Elastomer Adhesives," *Proc. of the IEEE Int. Conf. on Robotics and Automation*, pp. 2329-2335, 2006.

[8] M. Murphy and M. Sitti, "Waalbot: An Agile Small-Scale Wall Climbing Robot Utilizing Pressure Sensitive Adhesives," *IEEE/ASME Trans. on Mechatronics*, 2007, in press.

[9] K. Autumn, M. Buehler, et al., "Robotics in scansorial environments," *Proceedings of SPIE, Unmanned Ground Vehicle Technology VII*, vol. 5804, pp. 291-302, May 2005.

[10] F. Chiu, J. Guo, J. Chen, and Y. Lin, "Dynamic characteristic of a biomimetic underwater vehicle," *Proc. of the IEEE Int. Symposium on Underwater Technology*, pp. 172-177, 2002.

[11] S. Floyd, T. Keegan, and M. Sitti, "A novel water running robot inspired by basilisk lizards," *Proc. of the IEEE/RSJ Intelligent Robot Systems Conference*, pp. 5430-36, Beijing, China, Oct. 2006.

[12] D. L. Hu, B. Chan, and J. W. M. Bush, "The hydrodynamics of water strider locomotion," *Nature*, vol. 424, pp. 663-666, 2003.

[13] S. H. Suhr, Y. S. Song, S. J. Lee, and M. Sitti, "Biologically inspired miniature water strider robot," *Proc. of the Robotics, Science and Systems I*, pp. 319-325, 2005.

[14] Y. S. Song, S. H. Suhr, and M. Sitti, "Modeling of the supporting legs for designing biomimetic water strider robots," *Proc. of the Int. Conf. on Robotics and Automation*, pp. 2303-2310, Orlando, FL, 2006.

[15] Y. S. Song and M. Sitti, "Surface tension driven biologically inspired water strider robots: Theory and experiments," *IEEE Trans. on Robotics*, 2007, in press.